Nanoscale zero-valent iron particles for the remediation of plutonium and uranium contaminated solutions

Richard A. Crane,[1*] *Michelle Dickinson*[2] *and Thomas B. Scott*[2]

[1] School of Civil and Environmental Engineering, University of New South Wales, Australia

2 Interface Analysis Centre, School of Physics, University of Bristol, UK.

*Corresponding Author. E-mail: R.Crane@unsw.edu.au

Tel: 0117 331 1176

Keywords

21 Plutonium, zero-valent iron, nanoparticles, remediation, uranium

22

Abstract

In the current work the uptake of plutonium onto nanoscale zero-valent iron nanoparticles (nZVI) under anoxic conditions has been investigated. A uranyl solution was also studied under similar geochemical conditions to provide a comparative dataset. Following nZVI addition, a rapid and significant decrease in aqueous actinide concentration was recorded for both systems. The removal rate recorded for plutonium was slower, with 77 % removal recorded after 1 hour of reaction, compared to 99 % recorded for uranium. Low aqueous contaminant concentrations (<25 %) were then recorded for both systems until the end of the 7 day reaction period. XPS confirmed contaminant uptake onto the nZVI. For the plutonium system, the recorded photoelectron spectra exhibited Pu 4f lines centred at ~439 eV and ~427 eV, characteristic of Pu^{4+} and implying that chemical reduction of the sorbed plutonium had occurred, ascribed to the formation of PuO_2. Similarly, with the U-system, the recorded U 4f photoelectron peaks were centred at energies of ~380 eV and ~391 eV, characteristic of U^{4+} in UO_2. Results provide clear evidence that nZVI may be used as an effective material for the removal of plutonium from contaminated waters.

1. **Introduction**

To date, a principal environmental legacy of mankind's military and civil nuclear activities has been the discharge, either authorised or accidental, of many long-lived radionuclides. Actinides and other radionuclides present a considerable long-term environmental concern and have a strong bearing on the potential for site redevelopment. In addition, the contamination of groundwater by more soluble radionuclides can compromise drinking water sources and spread contamination over significant distances.

Within most civil nuclear reactors uranium dioxide (UO_2) is the primary fuel. However, transmutation of non-fissile ^{238}U also generates plutonium which contributes significantly to the overall energy output. This has been estimated to be up to 30 % from a pressurised water reactor (PWR) during its lifetime. [1] Furthermore, plutonium present in spent nuclear fuels has, in some countries, been separated for subsequent use in mixed oxide fission fuels or nuclear weapons. [1] Consequently, there exist several sites worldwide where plutonium contamination is a significant problem. Perhaps most notable is the Mayak nuclear reprocessing plant in the Russian Federation where, as a result of several decades of nuclear fuel reprocessing, plutonium storage and the 1957 Kyshtym disaster, soil and vegetation activities of up to several MBq m^{-2} have been recorded across the site. [2] The considerable radioactivity of the plutonium isotopes means that inventories of $^{239+240}Pu$ at Mayak have consistently contributed several kBq m^{-2}, [2],[3] a significant fraction of the total site radiation levels. In the UK, elevated radioactivity has previously been recorded for water samples taken in proximity to the Sellafield nuclear reprocessing plant in Cumbria, England. For example, a study in 1999

reported $^{239+240}$Pu concentrations in Scottish waters several hundred miles from the site up to73 mBq m^{-3}. [4]

The most important chemical property which governs the behaviour and fate of plutonium in groundwater systems is generally considered to be its oxidation state. In the environment, plutonium can exist as either: Pu^{3+}, Pu^{4+}, Pu^{5+} or Pu^{6+}. Under oxidising conditions, Pu^{5+} and Pu^{6+} are most common whereas, in chemically reducing conditions, Pu^{3+} and Pu^{4+} typically predominate. [5] In reality, the environmental prediction of plutonium valence is far from routine because all four oxidation states can exist in one single groundwater sample. [5] In conditions that typically exist in surface water systems (pH >6.5 and positive Eh), Pu^{4+}, Pu^{5+} and Pu^{6+} are the most common, [6],[7] with Pu^{4+} the most common valence state when sorbed. [7] Plutonium is also recognised to readily form complexes with various organic ligands, such as acetate, citrate, formate, fulvate, humate, lactate, oxalate and tartrate, with many inorganic ligands, such as hydroxyl, carbonate, nitrate, sulphate, phosphate, chloride, bromide and fluoride, and with many synthetic organic ligands, e.g. EDTA and 8-hydroxyquinoline derivatives. [8] Carbonate and bicarbonate are common anions in many natural water systems and form extremely stable aqua-complexes with plutonium and actinide ions in general. [9] Consequently, in natural waters the bulk of any dissolved plutonium is often comprised of plutonium-carbonate complexes. For example, a typical aerated groundwater sample at pH >6.5 is likely to be comprised of ~90 % $Pu(OH)_2(CO_3)_2^{2-}$ species with a minor percentage of $Pu(OH)_{4(aq)}$, [8] the latter compound tending to polymerise irreversibly. [10],[11] As a consequence, plutonium in the environment can be in aqueous, solid or colloidal forms. [12],[13] For example, Kersting et al., (1999) [14] documented the unexpected appearance of plutonium down-gradient from a known leakage source and showed that plutonium was transported in association with the colloidal fraction consisting of clays

(namely illite and smectite) and zeolites (namely mordenite and clinoptilolite/heulandite). Despite such work, there remains significant residual uncertainty with regard to the environmental fate of plutonium in the natural environmental and more specifically how plutonium interacts with geologic materials. [15]

A new and potentially potent tool for the clean-up of radionuclide contaminated waters is nanoscale zero-valent iron particles (nZVI). Compared to the granular ZVI more commonly used in permeable reactive barriers (ZVI particulates >1 μm in diameter), nZVI have a significantly greater surface area to volume ratio, and resultantly, a significantly higher rate of chemical reaction (corrosion). [16] The small size also allows the deployment of nZVI via injection for the *in situ* source treatment of contaminant plumes. [16] To date, nZVI have been investigated for the immobilisation of a range of metal and metalloid contaminant species, including transitions metals, such as: chromium, [17] cobalt, [18] copper, [19],[20], molybdenum, [20] nickel, [21], silver, [21] technetium [22], vanadium [23] and zinc [21]; post transition metals, such as: cadmium [21] and lead; [21],[24] and metalloids, such as: arsenic [25] and selenium [26]. Investigations for the remediation of radionuclides, however, remains less widely researched and includes: barium, [27], pertechnetate [21],[22] and uranium. [20],[28],[29],[30],[31],[32],[33],[34],[35] As demonstrated by Dickinson and Scott, (2010) [30], uranium uptake onto nZVI typically occurs via sorption and then surface-mediated chemical reduction. In comparison to the body of work reported for uranium, the uptake of plutonium by nZVI has not, as far as we are aware, been previously reported.

The current study aims to address this gap in research but does not, however, start from a position of complete ignorance with regard to Fe-Pu interactions. Indeed interactions between aqueous plutonium and iron-bearing minerals/materials are well documented,

with plutonium known to efficiently sorb to a range of iron (hydr)oxides, including hematite, ferrihydrite and goethite. [36] In addition many forms of plutonium are known to be redox active with regard to the ferrous iron. For example, aqueous Pu(V) has been documented to reduce to Pu(IV) when sorbed to hematite (α-Fe_2O_3) and goethite (α-FeOOH). [37] As a consequence an emerging field of research is the potential utility of engineered iron bearing materials as sorbents for plutonium. Additionally, as plutonium and uranium are often associated, a remediation technology that is effective for both radionuclides would be of great benefit. Correspondingly, this paper presents a preliminary study to assess the feasibility of using nZVI to remediate both plutonium and uranium contaminated solutions.

2. Materials and methods

2.1. Nanoparticle synthesis

nZVI were synthesised following an adaptation of the method first described by Wang and Zhang, 1997 [38], using sodium borohydride to reduce ferrous iron to a metallic state. Briefly, 7.65 g of $FeSO_4 \cdot 7H_2O$ were dissolved in 50 mL of Milli-Q water (resistivity 18.2 MΩ·cm at 25°C) and then a 4 M NaOH solution was used to adjust the pH to 6.8. The salts were then reduced to metallic nanoparticles by the addition of 3.0 g of $NaBH_4$. The nanoparticle product was isolated through centrifugation and then sequentially washed with water, ethanol and acetone (20 mL of each). The nanoparticles were dried in a desiccator under low vacuum (~10^{-2} mbar) for 48 hours and then stored in a nitrogen-filled glovebox until required.

2.2. Experimental procedure

All preparation and experimentation was performed in the oxygen-free nitrogen environment of a Saffron Scientific (Alpha series) glovebox under negative pressure. A Pu-solution of 1 ppm was synthesised by adding 0.3 mL of a 1000 ppm IRMM standard material to a 500 mL polypropylene bottle containing 300 mL of Milli-Q water. The U-solution was made by adding 0.3 mL of a 1000 ppm uranyl acetate stock solution into 300 mL of Milli-Q water. The pH of each system was measured and then 0.1 M NaOH was added dropwise to adjust both systems to pH 6. The systems were then left to equilibrate for a time period of 48 hours.

Prior to nanoparticle addition a 1 mL sample was taken from each batch system (time = 0 h) and the DO and Eh was measured and recorded. The 299 mL solutions were then divided into two smaller volumes of 99 mL and 200 mL to act as the experimental control and the sorption experiment, respectively. Two batches of nZVI (0.02 g each) were then added to 1 mL of absolute ethanol (Sigma Aldrich, ≥99.5%) and dispersed by sonication for 60 seconds using a Fisher Scientific Ultrasonic cleaner. The resultant slurry was then added to the batch systems, which were then gently agitated to disperse the nanoparticles throughout the sample.

Both systems were sampled at 1 h, 2 h, 4 h, 24 h, 48 h and 7 d. Prior to sampling, the jars were gently shaken to ensure homogeneity and then a disposable pipette was used to extract a 1 mL volume of liquid/nanoparticle mix which was expelled into a 1.5 mL Eppendorf tube. Two Eppendorfs were filled in this way, the lids closed and the tubes centrifuged for two minutes at 10,000 RPM using an Eppendorf MiniSpin centrifuge. The supernatant was then poured off into a 10 mL beaker and the process was repeated until approximately 10 mL of liquid had been sampled. (The small volume of solution and sample aliquots was determined by the limitations inherent with working within a glovebox and by the safety considerations around handling plutonium and uranium). Half

of the liquid was taken for pH and ORP (oxidation reduction potential) measurements, using a Hanna Instruments meter (model HI 8424) with a combination gel electrode pH probe and a platinum ORP electrode (model HI 3230B), respectively. The aqueous samples collected were then filtered through a 0.22 μm cellulose acetate filter and stored with a drop of concentrated HNO_3 prior to further preparation for inductively coupled plasma mass spectrometry (ICP-MS) analysis. The solids were rinsed sequentially in 2 mL each of water, acetone and then ethanol to remove any physi-sorbed species and residual water. At each sampling period the water rinse was also prepared for ICP-MS in order to study the physi-sorbed species. Solid samples were prepared by pipetting an acetone suspension of a small volume of material onto a copper stub for X-ray photoelectron spectroscopy (XPS) analysis and allowing them to dry under a vacuum of 1×10^{-2} mbar.

2.3. Sample analysis methods

2.3.1. ICP-MS preparation and conditions

Samples were prepared for ICP-MS by a 100 times dilution in 1 % nitric acid (analytical quality concentrated HNO_3 in Milli-Q water). Blanks, plutonium and uranium standards at 0.1, 0.25, 0.5, 1, 5 and 10 ppb were also prepared in 1 % nitric acid. An internal bismuth standard of 10 ppb was also added to all blanks, standards and samples. The ICP-MS instrument used was a VG Thermo Elemental PQ3.

2.3.2. TEM instrument conditions

TEM images were obtained with a JEOL JEM 1200 EX Mk 2 TEM, operating at 120 keV. The nZVI samples were mounted on 200 mesh holey carbon coated copper grids.

2.3.3. XRD instrument conditions

A Phillips Xpert Pro diffractometer with a $Cu_{K\alpha}$ radiation source (λ = 1.5406 Å) was used for XRD analysis (generator voltage of 40 keV; tube current of 30 mA). XRD spectra were acquired between 2θ angles of 0–90°, with a step size of 0.02° and a 2 s dwell time.

2.3.4. XPS instrument conditions

A Thermo Fisher Scientific Escascope equipped with a dual anode X-ray source ($Al_{K\alpha}$ 1486.6 eV and $Mg_{K\alpha}$ 1253.6 eV) was used for XPS analysis. Samples were analysed at $<5\times10^{-8}$ mbar with $Al_{K\alpha}$ radiation of 300 W (15 kV, 20 mA) power. High resolution scans were acquired using 30 eV pass energy and 300 ms dwell time. Following the acquisition of survey spectra over a wide binding energy range, the Fe2p, C1s, O1s, Pu4f and U4f spectral regions were then scanned at a higher energy resolution such that valence state determinations could be made for each element. Data analysis was carried out using Pisces software (Dayta Systems Ltd) with binding energy values of the spectra were referenced to the adventitious hydrocarbon C1s peak at 284.8 eV. In order to determine the relative proportions of Fe^{2+} and Fe^{3+} in the sample analysis volume, curve fitting of the recorded Fe2p photoelectron peaks was performed following the method of Grosvenor et al., 2004. [39] The Fe2p profile was fitted using photoelectron peaks at 706.7, 709.1, 710.6 and 713.4 eV corresponding to Fe^{0}, $Fe^{2+}_{octahedral}$, $Fe^{3+}_{octahedral}$ and $Fe^{3+}_{tetrahedral}$, respectively. These parameters were selected on the basis that the surface oxide was assumed to be a mixture of wüstite and magnetite, as the oxide Fe^{2+} is in the same coordination with the surrounding oxygen atoms in both forms of oxide.

3. Results and discussion

3.1. Preliminary characterisation of the nZVI

Preliminary characterisation of the nZVI was performed using BET surface area analysis, TEM, XRD and XPS. The physical and chemical properties of nZVI has been extensively characterised elsewhere. [40] Briefly, BET surface area recorded the nZVI as exhibiting a specific surface area of 14.8 m^2 g^{-1}. TEM analysis (Figure 1) determined that the nZVI are roughly spherical and loosely aggregated into chains and rings (when dry), a feature attributed to electrostatic and/or magnetic attraction forces between individual nanoparticulates. [16] XRD analysis (Figure 2a) confirmed that the nZVI consisted principally of poorly crystalline/amorphous metallic α-Fe with bcc structure. XPS analysis (Figure 2b) recorded a Fe^0/Fe^{2+} + Fe^{3+} ratio of 0.02, indicating that the surface oxide layer of the nZVI extended through the majority of the XPS analysis depth, which is approximately 5nm for Fe oxide materials. [40] Indeed, previous TEM studies have documented the oxide thickness of nZVI to be approximately 3-5 nm. [40] A Fe^{2+}/Fe^{3+} ratio of 0.38 was also recorded, indicating that the oxide layer is comprised of a ferrous and ferric iron mixture, with a stoichiometry similar to magnetite (Fe_3O_4). A summary of the experimental results is presented in Table 1.

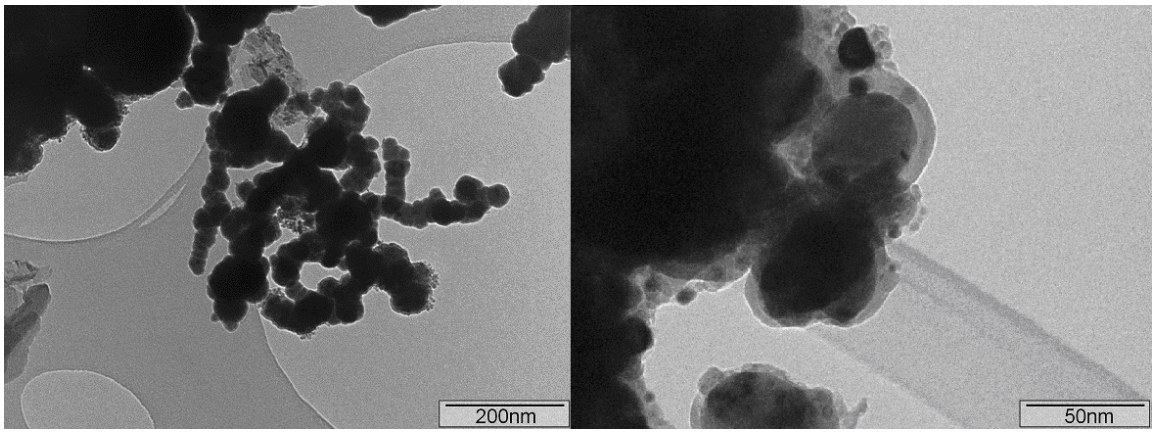

Figure 1. Transmission electron microscopy (TEM) images of the nZVI used in this study.

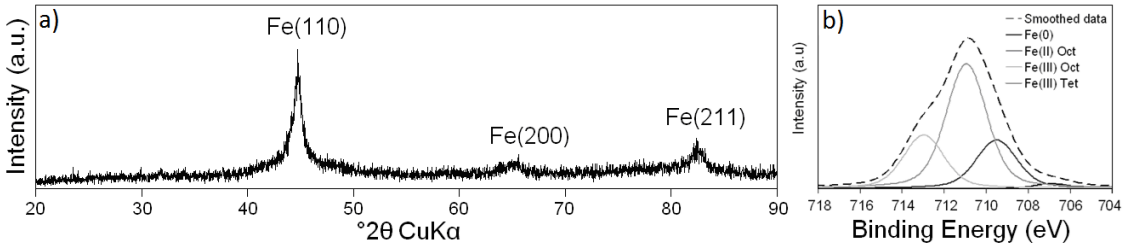

225

226 *Figure 2. X-ray diffraction (XRD) spectra for the range 20-90° 2θ (a); and X-ray photoelectron*

227 *spectroscopy (XPS) Fe $2p_{3/2}$ photoelectron spectra of the nZVI.*

228

Particle size distribution (%)	0-50 nm	85
	50-100 nm	8
	>100 nm	7
Oxide thickness (nm)		3-4
Surface area (m^2 g^{-1})		14.8
Surface composition (at. %)	Fe	30.5
	O	32.1
	C	14.5*
	B	22.9
Iron stoichiometry	$Fe^0/(Fe^{2+} + Fe^{3+})$	0.02
	Fe^{2+}/Fe^{3+}	0.38

229 *Table 1. A summary of the experimental results regarding the bulk and surface*

230 *properties of the nZVI. * It is likely that a high proportion of this is adventitious carbon.*

231 **3.2. Analysis of liquids**

232 **3.2.1. Changes in actinide concentration**

233 The plutonium and uranium concentrations, shown as percentages of the initial

234 concentrations, at different reaction times are shown in Figure 3. For the Pu-system the

235 initial concentration was significantly lower than the intended value of ~1 ppm; it was

236 measured at 64 ppb. This significantly reduced aqueous plutonium concentration was

237 ascribed to the adsorption of plutonium onto the clean walls of the reaction vessels and

238 glassware used for sample preparation. Following the study of Anderson et al., 2007,

[41] this was not an unexpected result. This previous study showed that up to 14% of total-Pu had sorbed to their reaction vessels. However, in the current work plutonium 'loss' was significantly greater than expected.

For the subsequent nZVI uptake experiments, the plutonium control systems indicated a similar adsorption phenomenon over the reaction period, with aqueous plutonium concentrations decreased to 53 % of initial values during the first two hours. This initial significant decrease is attributed to the transfer of the initial 300 mL of plutonium solution into the two smaller reaction vessels (a 200 mL nanoparticle experiment and 100 mL control) and the consequential sorption of plutonium onto the new vessels. After this period there was a slight, but less significant, decrease of plutonium concentration over the remaining time period implying that sorption to the vessel walls, or precipitation out of solution, continues to occur slowly over time. Correspondingly, in order to present the nZVI uptake results for plutonium more accurately, the initial decrease in plutonium concentration observed in the control system has been used to adjust the 0 h plutonium concentration in the nZVI sorption experiments, e.g. the initial 64 ppb plutonium concentration has been reduced by 53 % to become a more accurate initial aqueous value of 34 ppb.

Figure 3 displays the aqueous plutonium and uranium concentrations as a function of time for the 7 d reaction period. Following the addition of nZVI the concentration of both contaminants was recorded to decrease rapidly, with 77 and 99 % removal recorded for plutonium and uranium respectively at the 1 h sampling point. A further decrease in plutonium concentrations was then recorded throughout the 7 d reaction period. This occurred most rapidly during the initial stages, with 85 and 86 % removal recorded at the 2 and 4 h sampling points respectively. At the 24 h sampling point a relative plateau was reached with 90 % removal recorded, increasing to 91 % by the end of the 7 d sampling

period. In comparison, uranium removal was recorded to decrease slightly to 97 and 95 % respectively for sampling points at 2 and 4 hours respectively. A further gradual increase was then recorded with 84 % uptake recorded for the 7 d sampling point. It can therefore be concluded that both contaminants exhibited similar trends, in general, for their removal onto nZVI, with rapid and significant initial uptake (sampling periods $\leq$ 4 h), followed by significant retention of the sorbed actinides. It can also be noted, however, that the kinetics of plutonium uptake was much slower than uranium, and also no re-release was recorded for the former actinide specie whilst some re-release was recorded for the latter specie. With the surface area of nZVI assumed as the same for both systems this behaviour could be attributed to the aforementioned significantly higher starting concentration of uranium in comparison to plutonium. One further explanation could be related to any differential sorption affinities of the two actinides. For example, it is likely that for the starting redox conditions and pH tested in the current work (Eh = 185, pH = 6) plutonium and uranium would have been present predominantly as $Pu(OH)_3^+$ and UO_2^{2+} respectively, [42] with a lower sorption affinity likely to have been exhibited by the former species since it is a singly charged ion. [43] In addition, the partial re-release of uranium in comparison to the full plutonium retention recorded could also be related to differential chemical transformation (once sorbed) of the actinides. For example, uncomplexed pentavalent and hexavalent plutonium species are typically more easily chemically reduced than uranyl (UO_2^{2+}), and would therefore be more easily transformed into a more stable surface-bound state. [44]

A final consideration is that during the 7 day reaction period, the surface area of the nZVI would have changed due to progressive corrosion of the particles to form iron oxy-hydroxide products. This is assumed to have resulted in a progressive increase in the

available reactive surface area, which would in turn have encouraged further Pu adsorption.

3.2.2. Changes in pH and Eh

Prior to nanoparticle addition, the pH of both systems was measured as 6.0. The Eh and dissolved oxygen content were also measured as 185 mV and 3.18 mg L^{-1}, for the Pu-system and 186 mV and 4.43 mg L^{-1} for the U-system. Following the addition of the nZVI, an increase in solution pH was recorded, reaching a maximum of pH 10.5 and pH 9.35 in the Pu- and U-systems, respectively, Figure 3. Concurrent with this was a decrease in solution Eh, reaching minimum values of -233 mV after 1 h for the Pu-system and -294 mV after 2 h for the U-system, Figure 3. This behaviour is attributed to the rapid aqueous oxidation of the surface of the metallic iron nanoparticles (Eq. 1-4). The primary components available for corrosion reactions would have likely been dissolved oxygen (DO) and water itself, with the former being strongly thermodynamically favoured (Eq. 1).

$$2Fe^{0}_{(s)} + 4H^{+}_{(aq)} + O_{2(aq)} \rightarrow 2Fe^{2+} + 2H_2O_{(l)} \qquad E^0 = +1.67\ V \quad \text{(Eq. 1)}$$

$$2Fe^{0}_{(s)} + 2H_2O_{(l)} \rightarrow 2Fe^{2+} + H_{2(g)} + 2OH^{-}_{(aq)} \qquad E^0 = -0.39\ V \quad \text{(Eq. 2)}$$

Ferrous iron (Fe^{2+}) is the primary product from these reactions and, in turn, can undergo further oxidative transformation (Eq. 3 and 4).

$$Fe^{2+}_{(s)} + 2H^{+}_{(aq)} + \tfrac{1}{2}O_{2(aq)} \rightarrow 2Fe^{3+}_{(aq)} + H_2O_{(l)} \qquad E^0 = +0.46\ V \quad \text{(Eq. 3)}$$

$$2Fe^{2+}_{(s)} + 2H_2O_{(l)} \rightarrow 2Fe^{3+} + H_{2(g)} + 2OH^{-}_{(aq)} \qquad E^0 = -1.60\ V \quad \text{(Eq. 4)}$$

As a result of these corrosion mechanisms the nZVI would have been an active and dynamic source of various corrosion products, which may have included $Fe(OH)_2$,

311 $Fe(OH)_3$, Fe_3O_4, Fe_2O_3, FeOOH, $Fe_5HO_8 \cdot 4H_2O$ and green rusts. It is likely that the
312 formation of these corrosion product(s) and the aforementioned chemically reducing
313 conditions would have been responsible for the physical removal (sorption or
314 enmeshment) and in some instances chemical reduction of the exposed aqueous
315 plutonium and uranium species. It must be noted that whilst Eq. 1 and 2 are useful for
316 illustrative purposes that it would have been highly unlikely that quantitative removal of
317 either plutonium or uranium would have occurred directly on Fe^0 surfaces due to its
318 extremely low aqueous stability. Instead it is likely that the contaminants would have
319 been sorbed onto structural and/or precipitate ferrous or ferric iron species. [16]

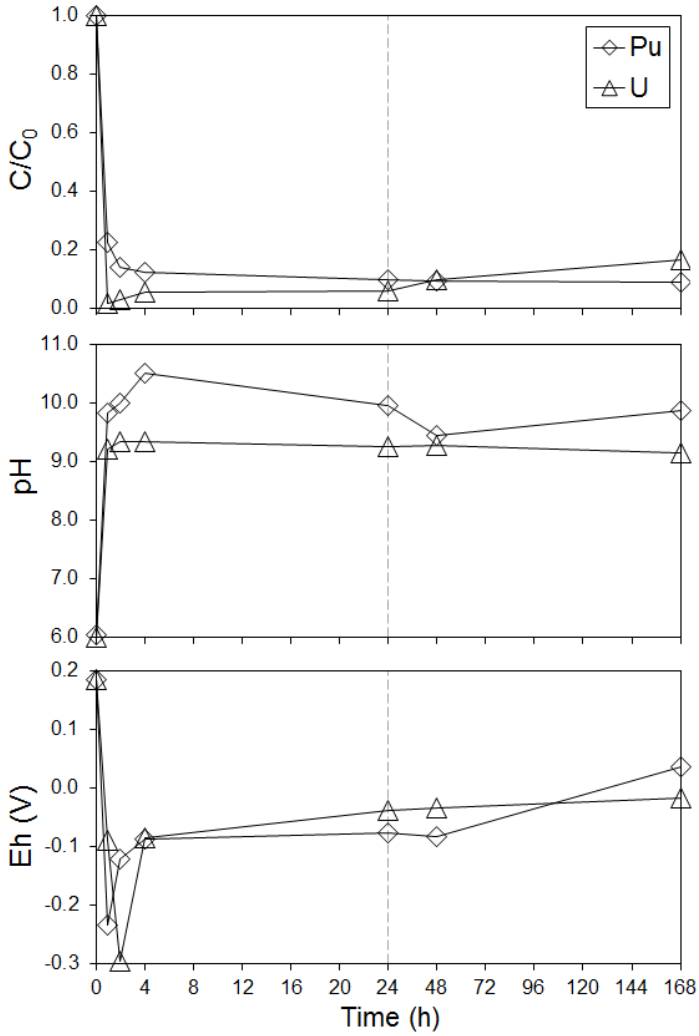

320

Figure 3. Actinide concentration, pH and Eh for the batch systems containing Pu- and U-systems at reaction times of 0h, 1h, 2h, 4h, 24h, 48h and 168h.

Analysis of the Milli-Q water used to rinse the nanoparticles from the Pu-system is shown in Figure 4. The low concentration typically recorded suggests that the majority of the sorbed Pu was chemi-sorbed (in a chemically reduced state) upon the nanoparticle surfaces.

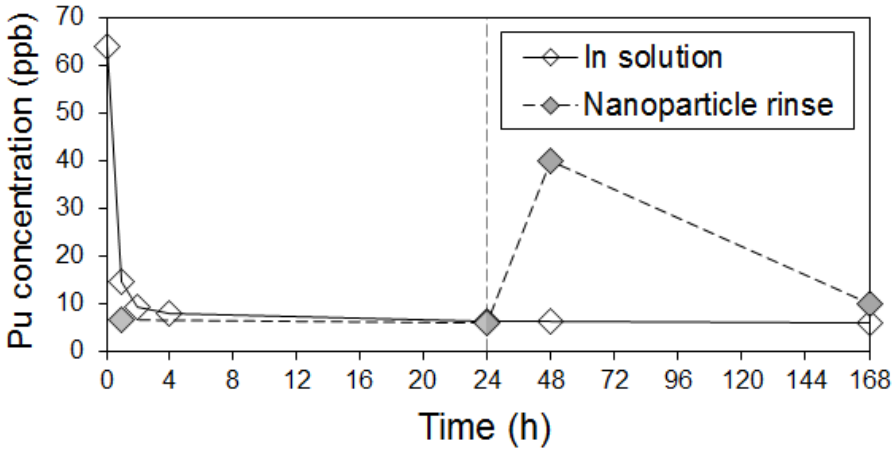

Figure 4. Plutonium concentration (ppb) in solution and in the nanoparticle rinse water.

3.3. Analysis of reacted nanoparticulate solids

XPS Fe $2p_{3/2}$ spectra of the unreacted nZVI and extracted samples taken at periodic intervals (1 h, 24 h, 48 h and 7 d) during the experiment is displayed in Figure 5. Analysis of the unreacted nanopowder using XPS recorded a Fe $2p_{3/2}$ photoelectron peak, centred at 710.3 eV (±0.3 eV), characteristic of a mixed-valence iron oxide (such as magnetite). A shoulder was also recorded on the low energy side of the primary peak, centred at 706.9 eV (±0.3 eV) indicating the presence of metallic iron, Fe^0. XPS analysis of the nanopowder extracted during the sorption experiment from both systems recorded

339 an increase in the binding energies of the $Fe2p_{3/2}$ profiles throughout the 7 day reaction
340 period, which is ascribed to the oxidation of the surface oxide from Fe^{2+} to Fe^{3+}. Analysis
341 of the O1s photoelectron peak for the standard (unreacted) nanopowder recorded a broad
342 peak centred at ~530.2 eV, indicating the presence of chemi-sorbed OH^- groups on the
343 surface of the nZVI prior to reaction. A shoulder peak was also recorded on the lower
344 binding energy side (~529.8 eV), representing O within the surface iron oxide layer.
345 Analysis of nanoparticulate solids taken during the reaction from both systems recorded
346 an increase in the contribution of the sorbed OH^- concurrent with a decrease in the iron
347 oxide contribution, with a shift in the O1s peak to ~530.9 eV recorded for both systems,
348 confirming the oxidation of the nanoparticle surfaces during the experiment.

349 For the nanoparticulate solids taken from the solution containing aqueous plutonium, the
350 binding energy region between 420 eV and 445 eV was scanned to determine whether
351 plutonium could be detected to confirm that was present on the nanoparticles. Although
352 the intensity of the photoelectron signal was often quite low, plutonium was identified on
353 all nanoparticulate samples from the sampled time periods. The central peaks were
354 located at ~439 eV and ~427 eV but the signal intensities were insufficient to permit
355 reliable curve-fitting. Larson, (1980) [45] reported the XPS binding energy of plutonium
356 within PuO_2 as between 426.1eV and 426.7eV. Consequently, the recorded peak energies
357 in the present study are typical of those previously reported for PuO_2. This provides
358 direct evidence to indicate that a considerable proportion of the plutonium removed on
359 the nanoparticle surfaces was in a tetravalent state. Furthermore, this implies that a
360 chemical reduction of the sorbed plutonium has occurred, which is ascribed to a coupled
361 redox reaction with Fe^{2+} at the nanoparticle surfaces, similar to the reaction mechanism
362 previously observed for aqueous uranium [46],[44]. For the nanoparticulate solids taken
363 from the solution containing aqueous uranium, the binding energy region between 374

eV and 396 eV was scanned to determine the presence and valence state of any uranium present on the nanoparticle surfaces. Again, uranium was identified on all nanoparticulate samples from the sampled time periods. The central peaks were located at ~380.1 eV (±0.2 eV) and ~391.2 eV (±0.2 eV), comparing well with values previously reported for non-stoichiometric UO_2, commonly referred to as UO_{2+x}, where $x \leq 2$. [47] Results from curve fitting following the method of Scott et al., (2008) [47] recorded a U^{4+}/U^{6+} ratio of 0.64 after 1 hour reaction, 0.61 after two hours of reaction, 0.74 after 24 hours of reaction and 0.79 after 7 days reaction. This provides clear evidence of rapid and sustained chemical reduction of U^{6+} to U^{4+} on the surface of the nZVI throughout the 7 day reaction period.

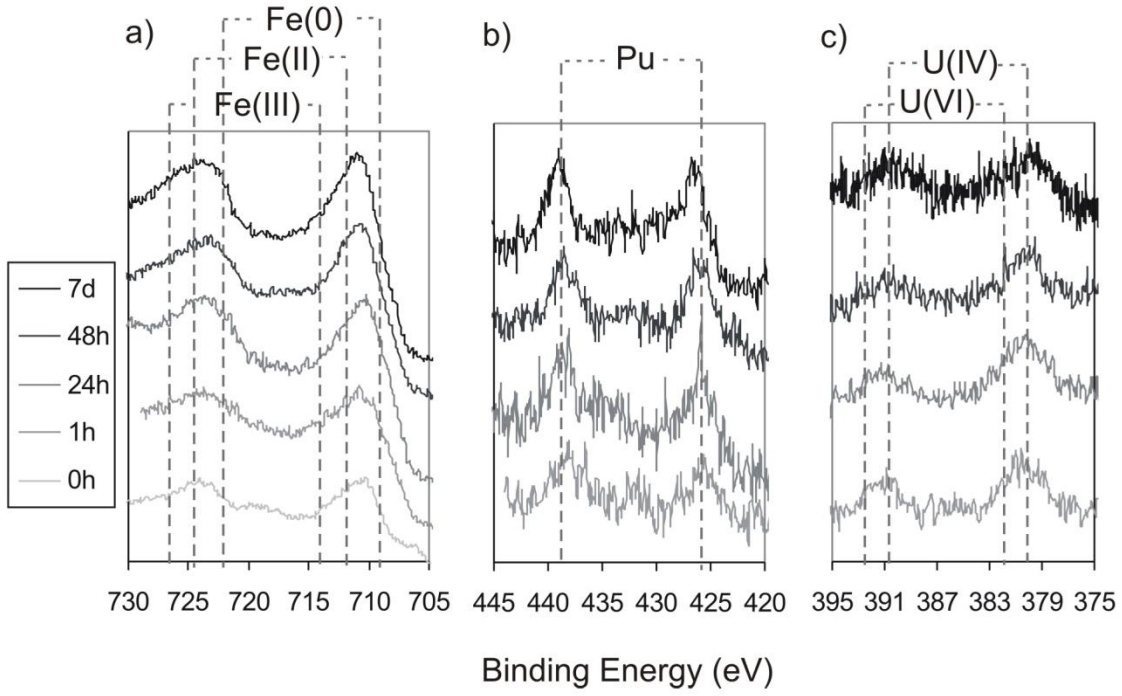

Figure 5. Photoelectron spectra acquired from nZVI taken from the batch systems after 0h, 1h, 24h, 48h and 168h: a) Fe2p from the Pu system; b) Pu4f from the Pu-system; and c) U4f from the U-system.

The results displayed here provide an indication the nZVI may be successfully utilised as a material for scavenging actinides from water. However, significant further research and development is required in order to achieve a technology that may be simply and reliably deployed and then subsequently recovered. One specific avenue for investigation is the development of composite filter materials in which nZVI may be incorporated as a reactive material, potentially alongside others. In such a structure the nZVI would be trapped or anchored such that the reactive properties are still exploited but the particles are immobilised. In this way the scavenged actinides may be efficiently recovered after being concentrated on the filter surfaces.

3.4. Potential utility of nZVI as a sorbent for plutonium and uranium

To date a wide array of sorbent materials have been investigated for the removal of plutonium and uranium from waste water, including titania microspheres [48], silica gel [49, transitional metal oxides [50], [51] and activated carbon [51]. The results presented in the current work demonstrate nZVI as effective for both plutonium and uranium removal; however, a direct comparison with the aforementioned conventional actinide sorbent materials cannot be drawn due to differences in experimental setup between the studies. It is clear, however, that a key advantage of nZVI is their ability to be suspended in solution as a colloid for maximum actinide scavenging and then recovered via magnetic attraction. This unique deployment and recovery mechanism could prove of considerable benefit for the treatment of radionuclide bearing waste streams where the magnetic nanoparticles (and sorbed radionuclides) can be efficiently recovered in a one-step and automated process, and then directly vitrified or stripped for re-use. There reuse efficacy, however, will depend on the concentration of dissolved oxygen in the batch treatment solutions. Time periods in the order of hours (approximately <48 hours) are typical for the transformation of nZVI into non paramagnetic (hydr)oxides in oxygenated

404 water compared to significantly longer time periods (e.g. >28 days) for anoxic systems.
405 [52]

406 **4. Conclusions**

407 The current work has provided a preliminary investigation of the mechanisms and
408 kinetics of the uptake of aqueous plutonium and uranium onto nanoscale zero-valent iron
409 particles. Following the addition of the nZVI to separate batch systems containing
410 plutonium and uranium, a rapid and significant decrease in aqueous concentrations were
411 recorded for both actinide species. Low aqueous contaminant concentrations (<25 %)
412 were then recorded for both systems until the end of the 7 day reaction period. Analysis
413 of extracted nanoparticulate solids using XPS confirmed the uptake of the contaminants
414 onto the nZVI. For the plutonium system, the recorded photoelectron spectra exhibited
415 Pu4f lines centred at ~439 eV and ~427 eV, characteristic of PuO_2. Similarly, with the U-
416 system U4f photoelectron peaks were recorded centred at energies of ~380 eV and ~391
417 eV, characteristic of UO_2. Results therefore indicate a removal mechanism for both
418 actinide species of sorption followed by chemical reduction on nZVI surfaces. Further
419 work will be aimed at determining the extent of chemical reduction more precisely.

420 **6. Acknowledgements**

421 The authors would further like to thank Mr Philip Purdie and Dr Sean Amos at the AWE
422 for facilitating the project. Research was funded by AWE plc under contract no.
423 CDK0534/30002873 and the Engineering and Physical Sciences Research Council.

424 **7. References**

[1] P.D. Wilson. The nuclear fuel cycle. Oxford Science Publications. (1996). ISBN: 0-19-856540-2

[2] G.C. Christensen, G.N. Romanov, P. Strand, B. Salbu, S.V. Malyshev, T.D. Bergan, D. Oughton, E.G. Drozhko, Y.V. Glagolenko, I. Amundsen, A.L. Rudjord, T.O. Bjerk, B. Lind. Radioactive contamination in the environment of the nuclear enterprise 'Mayak' PA. Results

from the joint Russian-Norwegian field work in 1994. Sci. Total. Environ., 202 (1997), pp. 237-248

[3] F. Gauthier-Lafaye, L. Pourcelot, J. Eikenberg, H. Beer, G, Le Roux, L.P. Rhikvanov, P. Stille, P. Renaud, A. Mezhibor. Radioisotope contaminations from releases of the Tomsk-Seversk nuclear facility (Siberia, Russia). J. Environ. Radio., 99 (2008), pp. 680-693

[4] P.J. Kershaw, D. McCubbin, K.S. Leonard. Continuing contamination of north Atlantic and Arctic waters by Sellafield radionuclides. Sci. Total. Environ., 30 (1999), pp.119-132

[5] J.W. Morse, G.R. Choppin. The chemistry of transuranic elements in natural waters. Rev. Aqu. Sci., 4 (1991), pp. 1-22

[6] D.I. Kaplan, B.A. Powell, L. Gumapas, J.T. Coats, R.A. Fjeld, D.P. Diprete. Influence of pH on plutonium desorption/solubilization from sediment. Environ. Sci. Technol., 40 (2006), pp. 5937-5942

[7] G.R. Choppin, A. Morgenstern. Distribution and movement of environmental plutonium, in Plutonium in the environment, A. Kudo, ed., (2001), pp. 91-105. ISBN: 978-0-08-043425-4

[8] Environmental Protection Agency (1999) Understanding variation in partition coefficient, Kd, values. Volume II: Review of geochemistry and available Kd values for cadmium, cesium, chromium, lead, plutonium, radon, strontium, thorium, tritium (3H), and uranium. EPA 402-R-99-004B

[9] D.L. Clark, D.E. Hobart, M.P. Neu. Actinide carbonate complexes and their importance in actinide environmental chemistry. Chem. Rev., 95 (1995), pp. 25-48

[10] S.R. Ashton. Evaluation of the chemical forms of plutonium in seawater. Marine Chem., 8 (1980), pp. 319-325

[11] J.I. Kim, B. Kanellakopulopolos. Solubility products of Pu(IV) oxide and hydroxide. Radiochim. Acta., 48 (1989), pp. 145-150

[12] W. Runde, S.D. Conradson. D. Wes Efurd, N. Lu, C.E. VanPelt, C. Drew Tait. Solubility and sorption of redox-sensitive radionuclides (Np, Pu) in J-13 water from the Yucca Mountain site: Comparison between experiment and theory. App. Geochem., 17 (2002), pp. 837-853

[13] P. Toulhoat. Confinement and migration of radionuclides in a nuclear waste deep repository. Comptes Rendus Physique., 3 (2002), pp. 975-986

[14] A.B. Kersting, D.W. Efurd. D.L. Finnegan, D.J. Rokop, D.K. Smith, J.L. Thompson. Migration of Plutonium in Ground Water at the Nevada Test Site. Nature., 397 (1999), pp.56–59

[15] M.C. Duff. Speciation and transformations of sorbed Pu on geologic materials: Wet chemical and spectroscopic observations. Radio. Environ., 1, (2001), pp. 139-157

[16] R.A. Crane, T.B. Scott. Nanoscale zero-valent iron: future prospects for an emerging water treatment technology. J. Hazard. Mater., 211 (2012), pp. 112-125.

[17] Y. Xu, D. Zhao. Reductive immobilization of chromate in water and soil using stabilized iron nanoparticles. Water Res., 41 (2007), pp.2101–2108

[18] Ç. Üzüm, T. Shahwan, A.E. Eroğlu, I. Lieberwirth, T.B. Scott, K.R. Hallam. Application of zero-valent iron nanoparticles for the removal of aqueous Co2+ ions under various experimental conditions. Chem. Eng. J., 144 (2008), pp. 213–220

[19] D. Karabelli, Ç. Üzüm, T. Shahwan, A.E. Eroğlu, I. Lieberwirth, T.B. Scott, K.R. Hallam. Batch removal of aqueous Cu2+ ions using nanoparticles of zero-valent iron: a study of the capacity and mechanism of uptake. Ind. Eng. Chem. Res., 47 (2008), pp. 4758–4764

[20] T.B. Scott, I.C. Popescu, R.A. Crane, C. Noubactep. Nano-scale metallic iron for the treatment of solutions containing multiple inorganic contaminants. J. Hazard. Mater., 186 (2011), pp. 280–287

[21] S.M. Ponder, J.G. Darab, J. Bucher, D. Caulder, I. Craig, L. Davis, N. Edelstein, W. Lukens, H. Nitsche, L.F. Rao, D.K. Shuh, T.E. Mallouk. Surface chemistry and electrochemistry of supported zerovalent iron nanoparticles in the remediation of aqueous metal contaminants. Chem. Mater., 13 (2001), pp. 479–486

[22] J.G. Darab, A.B. Amonette, D.S.D. Burke, R.D. Orr. Removal of pertechnetate from simulated nuclear waste streams using supported zerovalent iron. Chem. Mater.,19 (2007), pp. 5703–5713

[23] S. Klimkova, M. Cernik, L. Lacinova, J. Filip, D. Jancik, R. Zboril. Zero-valent iron nanoparticles in treatment of acid mine water from in situ uranium leaching. Chemosphere., 82 (2011), pp. 1178–1184

[24] X-Q. Li, W-X. Zhang. Sequestration of metal cations with zerovalent iron nanoparticles: a study with high resolution X-ray photoelectron spectroscopy (HR-XPS). J. Phys. Chem., 111 (2007), pp. 6939–6946

[25] S.R. Kanel, B. Manning, L. Charlet, H. Choi. Removal of arsenic(III) from groundwater by nanoscale zero-valent iron. Environ. Sci. Technol., 39 (2005), pp. 1291–1298

[26] J.T. Olegario, N. Yee, M. Miller, J. Sczepaniak, B. Manning. Reduction of Se(VI) to Se(-II) by zerovalent iron nanoparticle suspensions. J. Nanopart. Res., 12 (2010), pp. 2057–2068

[27] O. Çelebi, Ç. Üzüm, T. Shahwan, H.N. Erten. A radiotracer study of the adsorption behavior of aqueous Ba^{2+} ions on nanoparticles of zero-valent iron. J. Hazard. Mater., 148 (2007), pp.761-767

[28] O. Riba, T.B., Scott, K.V. Ragnarsdottir, G.C. Allen. Reaction mechanism of uranyl in the presence of zero-valent iron nanoparticles, Geochim. Cosmochim. Acta., 72 (2008), pp. 4047-4057

[29] R.A. Crane, M. Dickinson, I.C. Popescu, T.B. Scott. Magnetite and zero-valent iron nanoparticles for the remediation of uranium contaminated environmental water. Water. Res., 45 (2011), pp. 2931-2942

[30] M. Dickinson, T.B. Scott. The application of zero-valent iron nanoparticles for the remediation of a uranium-contaminated waste effluent. J. Hazard. Mater., 178 (2010), pp. 171-179

[31] M. Dickinson, T.B. Scott. The effect of vacuum annealing on the remediation abilities of iron and iron-nickel nanoparticles. J. Nano. Res., 12 (2010), pp. 2081-2092

[32] R.A. Crane, T.B. Scott. The effect of vacuum annealing of magnetite and zero-valent iron nanoparticles on the removal of aqueous uranium. J. Nanotech., 2013 (2013), pp. 1-11.

[33] R.A. Crane, T.B. Scott. The removal of uranium onto nanoscale zero-valent iron particles in anoxic batch systems. J. Nanomater., 2014 (2014), pp. 1-9.

[34] I.C., Popescu, P. Filip, D. Humelnicu, I. Humelnicu, T.B. Scott, R.A. Crane. Removal of uranium (VI) from aqueous systems by nanoscale zero-valent iron particles suspended in carboxy-methyl cellulose. J. Nucl. Mater., 443 (2013), pp. 250-255

[35] S. Yan, B. Hua, Z. Bao, J. Yang, C. Liu, B. Deng. Uranium(VI) removal by nanoscale zerovalent iron in anoxic batch systems. Environ. Sci. Technol., 44 (2010), pp.7783-7789

[36] Triay, I. R., Lu, N., Cotter, C. R. & Kitten, H. D. Iron Oxide Colloid Facilitated Plutonium Transport in
Goundwater (Am. Chemical Soc., Las Vegas, 1997).

[37] Powell, B. A., Fjeld, R. A., Kaplan, D. I., Coates, J. T., Serkiz, S. M.: Environ. Sci. Technol. 39, 2107 (2005).

[38] C.B. Wang, W.X. Zhang. Synthesizing nanoscale iron particles for rapid and complete dechlorination of TCE and PCBs. Environ. Sci. Technol., 31 (1997), pp. 2154-2156

[39] A.P. Grosvenor, B.A. Kobe, M.C. Biesinger, N.S. McIntyre. Investigation of multiplet splitting of Fe 2p XPS spectra and bonding in iron compounds. Surf. Inter. Analy., 36 (2004), pp. 1564-1574

[40] T.B. Scott, M. Dickinson, R.A. Crane, O. Riba, G. Hughes, G.C. Allen. The effects of vacuum annealing on the structure and surface chemistry of iron nanoparticles., J. Nano. Res. 12 (2010), pp. 2081-2092.

[41] E.B., Anderson, Y.M., Rogozin, E.A., Smirnova, R.V. Bryzgalova, N.R. Andreeva, S.I. Malimonova, S.I. Shabalev, A. Fujiwara, O. Tochiyama. Sorption-barrier properties of granitoids and andesite-basaltic metavolcanites with respect to Am(III) and Pu(IV): 1. Adsorption of Am and Pu from groundwater on monolithic samples of granitoids and andesite-basaltic metavolcanites. Radiochem., 49 (2007), pp. 270-277

[42] G.R. Choppin. Actinide speciation in aquatic systems. Marine Chem., 99 (2006), pp. 83-92

[43] A. Bondiettie, T. Tamura. Physicochemical associations of plutonium and other actinides in soils. In: *Transuranic elements in the environment*. U.S. Department of Energy, National Technical Information Service; DOE/TIC-22800; 145-1 64; 1980.

[44] D.T. Reed, S.E. Pepper, M.K. Richmann, G. Smith, R. Deo, B.E. Rittmann. Subsurface bio-mediated reduction of higher-valent uranium and plutonium. J Alloy. Comp., 444-445 (2007), pp. 376–382

[45] D.T. Larson. AES and XPS study of plutonium oxidation. J. Vac. Sci. Technol., 17 (1980), pp. 55-59

[46] T.B. Scott, G.C. Allen, P.J. Heard, A.C. Lewis, D.F. Lee. The extraction of uranium from groundwaters on iron surfaces. Proc. R. Soc. A., 461 (2005), pp. 1247–1259

[47] T.B. Scott, G.C. Allen, P.J. Heard, M.G. Randall. Reduction of U(VI) to U(IV) on the surface of magnetite. Geochim. Cosmochim. Acta., 69 (2005), pp. 5639-5646

[48] I.C. Pius, R.D. Bhanushali, Y.R. Bamankar, S.K. Mukerjee, V.N. Vaidya. Removal of plutonium from carbonate medium using titania microspheres prepared by sol-gel route. J. Radio. Nucl. Chem., 261 (2004), pp. 547-550

[49] X.G. Liu, J.F. Liang, J.M. Xu. Study on the adsorption behavior of silica gel for zirconium, plutonium and other fission products in high-level liquid waste. J. Radio. Nucl. Chem., 273 (2007), pp. 49–54

[50] M.T. Crespo, J.L. Gasc6n and M.L. Acefia. Techniques and analytical methods in the determination of uranium, thorium, plutonium, americium and radium by adsorption on manganese dioxide. Sci. Total Environ., 130-131 (1993), pp. 383-391

[51] L.N. Oji, W.R. Wilmarth, D.T. Hobbs, Loading capacities for uranium, plutonium, and neptunium in high caustic nuclear waste storage tanks containing selected sorbents. Nucl. Technol., 169 (2010), pp. 143–149

[52] R.A. Crane, C. Noubactep. Elemental metals for environmental remediation: lessons from hydrometallurgy. Fresen. Env. Bull., 21 (2012), pp. 1192-1196.